

Computation of 2D anisotropic elastic Green's functions and their gradients

Nicolas Venkovic^{*1} and Lori Graham-Brady^{†1}

¹Department of Civil Engineering, Johns Hopkins University

September 25, 2017

Abstract

A semi-analytical recursive method to compute the gradients of arbitrary orders of the Green's functions of 2D anisotropic elastic media is proposed, implemented and validated. Following a polar representation of the 2D linear elastic stiffness tensor, analytical expressions of the Barnett-Lothe integrands and their derivatives are obtained for anisotropic, orthotropic, R_0 -orthotropic, square symmetric and isotropic media. Analytical expressions for the complete Barnett-Lothe integrals are only obtained for isotropic media. In the case of anisotropy and other elastic symmetries, those integrals are evaluated numerically. The recursive relations are derived making use of the fact that the separation between dependence on orientation and lag of the Green's functions remains true irrespectively of material symmetry (or lack of it). The method makes use of the complete Barnett-Lothe integrals and the derivatives of the corresponding integrands of orders increasing with the order of the gradients of interest. Verification and validation of the method are successfully carried over both analytically, and numerically.

Source Code

A library called `GreenAnisotropic2D` is developed in C++ and wrapped into a Python module. The source files are

- | | | |
|--|--|----------------------------|
| • <code>dG_recursive.cpp</code> | • <code>dkN2_orthotropic.cpp</code> | • <code>medium.cpp</code> |
| • <code>dkN1_anisotropic.cpp</code> | • <code>dkN2_r0_orthotropic.cpp</code> | • <code>README</code> |
| • <code>dkN1_orthotropic.cpp</code> | • <code>dkN2_square_symmetric.cpp</code> | • <code>set_sym.cpp</code> |
| • <code>dkN1_r0_orthotropic.cpp</code> | • <code>dkN2_isotropic.cpp</code> | • <code>setup.py</code> |
| • <code>dkN1_square_symmetric.cpp</code> | • <code>etc.cpp</code> | • <code>test.py</code> |
| • <code>dkN1_isotropic.cpp</code> | • <code>example.py</code> | • <code>wrapper.cpp</code> |
| • <code>dkN2_anisotropic.cpp</code> | • <code>GreenAnisotropic2D.hpp</code> | |

Details on how to compile and wrap the module as well as how to run the test cases can be found in the `README` file. A Mathematica script `GreenAnisotropic2D.wl` is provided along with the source code for some of the verification and validation.

Contents

1	Introduction	2
2	Polar representation of 2D anisotropic elastic stiffnesses	3
2.1	Anisotropy	3
2.2	Orthotropy	3
2.3	R_0 -orthotropy	4
2.4	Square symmetry	4
2.5	Isotropy	5
2.6	Generalized moduli and polar diagrams	5

^{*}nvenkov1@jhu.edu

[†]lori@jhu.edu

3	Green's functions for concentrated forces in a plane	5
4	2D Stroh formalism	6
4.1	Concentrated force applied at the origin	8
5	2D Barnett-Lothe integral formalism	9
6	Recursive expressions for the gradients of the Green's function	12
7	Symmetry-dependent results	14
7.1	Orthotropies	14
7.2	Square symmetry	14
7.3	Isotropy	14
8	Verification and validation	15
8.1	Global equilibrium	15
8.1.1	Random curves	15
8.1.2	Traction integration	16
8.2	Verification	16
9	Conclusion	18
	Brisard et al. (2014)	

1 Introduction

In another study, we derive estimates of stationary high order polynomial polarization stress fields of the Hashin-Shtrikman functional of heterogeneous anisotropic elastic media. Those estimates are obtained from a Taylor expansion of the integrand of the Hashin-Shtrikman functional. After appropriate change of variables, those estimates can be recast in series of inner products between Minkowski tensors of uniform phases (i.e. grains for polycrystals) and gradients of elastic anisotropic Green's functions evaluated away from the origin. Our first implementation of this other work being two-dimensional, we need to be able to evaluate those Green's functions in anisotropic planes. Although analytical expressions for the Fourier transform of such Green's functions are known, their evaluation and differentiation at specific points of the real plane is not trivial. Indeed, due to the singularity of the Fourier transform of these Green's functions at vanishing wave amplitudes, the numerical estimation of the inverse transform is not well-behaved. The problem has well documented solutions for three-dimensional cases in which the integral of the inverse transforms is recast into a well behaved line integrals; this can be done as in the appendix of (Synge, 1957), or using Radon transforms (Bacon et al., 1980). Building on these results, expressions of arbitrary gradients of the Green's function can be evaluated upon well-behaved numerical integration, see Barnett (1972), Willis (1975), Sales and Gray (1998) and Lee (2009). Meanwhile, a similar regularization of the two-dimensional inverse transforms of the Green's function and its gradients is, to the best of our knowledge and attempts, not possible. Consequently, another approach has to be used to compute the 2D Green's function of elastic anisotropic media and its gradients.

First, we look at the early work of Eshelby et al. (1953) who proposed a general framework to solve for two-dimensional displacement fields due to dislocations in anisotropic media. This method, further developed and popularized by Stroh (Stroh, 1958, 1962), allows to express displacement fields in terms of a superposition of complex functions weighted by *Stroh eigenvectors* and whose form depends on the boundary conditions. However, for some cases, the solution obtained is not complete and must be adjusted to properly solve for the displacement field, see Ting (1996). Those cases are the ones we refer to as *material degeneracies* and for which the Stroh eigenvectors are not independent. Thus, the simplest form of the solution obtained by the Stroh formalism being correct upon the condition of non-degeneracy of the elastic stiffness tensor, we find it more convenient to resort to the integral formalism proposed by (Barnett and Lothe, 1973) as it shows more robustness in regards of the material symmetry. In the Barnett-Lothe formalism, the displacement field due to concentrated forces and dislocations is expressed in terms of integrals which we refer to as complete and incomplete Barnett-Lothe integrals. For most cases, those integrals have to and can be evaluated numerically.

From the solution of the displacement field obtained by the Barnett-Lothe formalism, one can simply obtain an expression for the Green's function due to a concentrated force at the origin of an anisotropic plane. As mentioned before, our interest lies in estimating gradients of arbitrary order of the Green's functions rather than the function itself. Starting from a general expression of the Green's function, we find that its gradients can always be multiplicatively decomposed into a scalar function depending on the distance from the origin to the point of evaluation, and a tensorial part which depends only on the orientation of the vector linking these two points. From this observation, we derive recursive expressions for

the tensor-valued angle-dependent part of the gradients, the scalar part depending on the distance being trivial to solve for. Eventually, one has to evaluate the complete Barnett-Lothe integrals (numerically, except for isotropic cases) as well as derivatives of the integrand of those integrals of orders increasing with the order of the gradient of interest. Using a representation of 2D elastic stiffnesses in terms of polar invariants (Vannucci, 2016), we derive analytical expressions for the derivatives of the *Barnett-Lothe integrands* up to the seventh order allowing us to compute the gradients of Green's functions up to order eight. A recursive algorithm is then implemented to compute those gradients for the cases of anisotropic, orthotropic, R0-orthotropic, square symmetric and isotropic media. The method is validated analytically using *Mathematica*, and numerically.

2 Polar representation of 2D anisotropic elastic stiffnesses

As presented in Vannucci (2016), it is known that the elastic stiffness tensor of 2D anisotropic media can be represented in terms of polar invariants and some angles. The advantages of such a representation is an increased simplicity in identifying material symmetries through conditions expressed in simple algebraic expressions of those invariants. The Cartesian components of the stiffness tensors are expressed in terms of those invariants and some angles. Passive rotations of the tensor are then carried over by setting a shift angle in the expressions for those components, hence simplifying changes of coordinate frames. All the symmetry-specific derivations done in this project are carried over using this *polar representation* of the Cartesian components of the stiffness tensor.

2.1 Anisotropy

For anisotropic media, the following independent invariants exist: four polar moduli T_0, T_1, R_0, R_1 and $\Phi_1 - \Phi_0$, where Φ_0 and Φ_1 are referred to as polar angles. The Cartesian components of the stiffness are

$$\begin{aligned} L_{1111} &= T_0 + 2T_1 + R_0 \cos(4\Phi_0) + 4R_1 \cos(2\Phi_1), \\ L_{1112} &= R_0 \sin(4\Phi_0) + 2R_1 \sin(2\Phi_1), \\ L_{1122} &= -T_0 + 2T_1 - R_0 \cos(4\Phi_0), \\ L_{1212} &= T_0 - R_0 \cos(4\Phi_0), \\ L_{2212} &= -R_0 \sin(4\Phi_0) + 2R_1 \sin(2\Phi_1), \\ L_{2222} &= T_0 + 2T_1 + R_0 \cos(4\Phi_0) - 4R_1 \cos(2\Phi_1) \end{aligned}$$

where T_0 and T_1 are referred to as the isotropic polar invariants in opposition to R_0, R_1 and $\Phi_0 - \Phi_1$ which we call anisotropic polar invariants. The other components are trivially obtained when enforcing minor and major symmetries. Conveniently, passive rotations of a counter-clockwise angle θ are obtained by substituting Φ_j with $\Phi_j - \theta$. The conditions under which the strain energy of a linear elastic medium with such a stiffness is guaranteed are

$$\begin{aligned} T_0 - R_0 &> 0, \\ T_1(T_0^2 - R_0^2) - 2R_1^2\{T_0 - R_0 \cos[4(\Phi_0 - \Phi_1)]\} &> 0, \\ R_0 &\geq 0, \\ R_1 &\geq 0 \end{aligned}$$

which implies $T_0 > 0$ and $T_1 > 0$. Elastic symmetries are expressed in terms of conditions defined on algebraic expressions of the polar invariants. More precisely,

$$R_0 R_1^2 \sin[4(\Phi_0 - \Phi_1)] \neq 0$$

implies anisotropy. If under some conditions, the left-hand-side of the expression above does equate zero, the stiffness is symmetric. Clearly, one can identify at least three cases of elastic symmetry; first, if $R_0 = 0$, second, if $R_1 = 0$ and finally, if $\sin[4(\Phi_0 - \Phi_1)] = 0$.

2.2 Orthotropy

Orthotropy occurs when $\sin[4(\Phi_0 - \Phi_1)] = 0$ which implies $\Phi_0 - \Phi_1 = K\pi/4$ for $K = 0$ or 1 . Therefore, for a given set of invariants T_0, T_1, R_0 and R_1 , there *may* exist two distinct orthotropic media (keeping the requirement of positive strain energy in mind); one for $K = 0$ and another for $K = 1$. The Cartesian components of the stiffness are then given by

$$L_{1111} = (-1)^K R_0 \cos(4\theta) + 4R_1 \cos(2\theta) + T_0 + 2T_1,$$

$$\begin{aligned}
L_{1112} &= -(-1)^K R_0 \sin(4\theta) - 2R_1 \sin(2\theta), \\
L_{1122} &= -(-1)^K R_0 \cos(4\theta) - T_0 + 2T_1, \\
L_{1212} &= T_0 - (-1)^K R_0 \cos(4\theta), \\
L_{2212} &= (-1)^K R_0 \sin(4\theta) - 2R_1 \sin(2\theta), \\
L_{2222} &= (-1)^K R_0 \cos(4\theta) - 4R_1 \cos(2\theta) + T_0 + 2T_1
\end{aligned}$$

where θ indicates a passive counter-clockwise rotation. Here, K is also an invariant. Interesting properties of this invariant are documented in Vannucci (2009). Note that for $\theta = 0$ or $\pi/2$, we have $L_{1112} = L_{2212} = 0$. The conditions under which the strain energy of a linear elastic medium with such a stiffness is guaranteed are

$$\begin{aligned}
T_0 - R_0 &> 0, \\
T_1[T_0^2 + (-1)^K R_0] - 2R_1^2 &> 0, \\
R_0 &\geq 0, \\
R_1 &\geq 0.
\end{aligned}$$

2.3 R0-orthotropy

A special case of orthotropy is obtained when $R_0 = 0$, namely R0-orthotropy. The Cartesian components of the corresponding stiffness can be cast in the form

$$\begin{aligned}
L_{1111} &= 4R_1 \cos(2\theta) + T_0 + 2T_1, \\
L_{1112} &= -2R_1 \sin(2\theta), \\
L_{1122} &= -T_0 + 2T_1, \\
L_{1212} &= T_0, \\
L_{2212} &= -2R_1 \sin(2\theta), \\
L_{2222} &= -4R_1 \cos(2\theta) + T_0 + 2T_1
\end{aligned}$$

where L_{1122} and L_{1212} are isotropic. Note that irrespectively we have $L_{1112}(\theta) = L_{2212}(\theta)$ for all θ . Also, for $\theta = 0$ or $\pi/2$, we still have $L_{1112} = L_{2212} = 0$. The conditions under which the strain energy of a linear elastic medium with such a stiffness become

$$\begin{aligned}
T_0 &> 0, \\
T_1 T_0^2 - 2R_1^2 &> 0, \\
R_1 &\geq 0.
\end{aligned}$$

2.4 Square symmetry

Square symmetry occurs when $R_1 = 0$. The Cartesian components of the stiffness are then given by

$$\begin{aligned}
L_{1111} &= T_0 + 2T_1 + R_0 \cos(4\theta), \\
L_{1112} &= -R_0 \sin(4\theta), \\
L_{1122} &= -T_0 + 2T_1 - R_0 \cos(4\theta), \\
L_{1212} &= T_0 - R_0 \cos(4\theta), \\
L_{2212} &= R_0 \sin(4\theta), \\
L_{2222} &= T_0 + 2T_1 + R_0 \cos(4\theta).
\end{aligned}$$

The conditions under which the strain energy of a linear elastic medium with such a stiffness is guaranteed are

$$\begin{aligned}
T_0 &> 0, \\
T_1(T_0 - R_0) &> 0, \\
R_0 &\geq 0.
\end{aligned}$$

2.5 Isotropy

The Cartesian components of an isotropy elastic stiffness can be expressed as follows in terms of the polar invariants T_0 and T_1

$$\begin{aligned} L_{1111} &= T_0 + 2T_1, \\ L_{1112} &= 0, \\ L_{1122} &= -T_0 + 2T_1, \\ L_{1212} &= T_0, \\ L_{2212} &= 0, \\ L_{2222} &= T_0 + 2T_1 \end{aligned}$$

so that the following relations exist with the usual elastic moduli of a plane

$$T_0 = \mu_{2D} \quad \text{and} \quad 2T_1 = \kappa_{2D}$$

where μ_{2D} and κ_{2D} are the planar shear and bulk moduli, respectively. The conditions under which the strain energy of a linear isotropic elastic medium is non-negative are $T_0 > 0$ and $T_1 > 0$.

2.6 Generalized moduli and polar diagrams

Following Hayes (1972), we can compute generalized elastic moduli as follows. First, the elongation stiffness along a unit vector \underline{m} is given by

$$E(\theta) = ([\underline{m}(\theta) \otimes \underline{m}(\theta)] : \mathbb{L}^{-1} : [\underline{m}(\theta) \otimes \underline{m}(\theta)])^{-1} \quad (1)$$

whereas the generalized shear modulus is defined using a vector \underline{p} orthogonal to \underline{m} :

$$\mu(\theta) = (4[\underline{m}(\theta) \otimes \underline{p}(\theta)] : \mathbb{L}^{-1} : [\underline{m}(\theta) \otimes \underline{p}(\theta)])^{-1}. \quad (2)$$

The generalized Poisson's ratio is given by

$$\nu(\theta) = -\frac{[\underline{p}(\theta) \otimes \underline{p}(\theta)] : \mathbb{L}^{-1} : [\underline{m}(\theta) \otimes \underline{m}(\theta)]}{[\underline{m}(\theta) \otimes \underline{m}(\theta)] : \mathbb{L}^{-1} : [\underline{m}(\theta) \otimes \underline{m}(\theta)]}. \quad (3)$$

The following isotropic averages are introduced for a better illustration of material symmetries:

$$E = \frac{1}{2\pi} \int_0^{2\pi} E(\theta) d\theta, \quad \mu = \frac{1}{2\pi} \int_0^{2\pi} \mu(\theta) d\theta, \quad \nu = \frac{1}{2\pi} \int_0^{2\pi} \nu(\theta) d\theta. \quad (4)$$

Obviously, for isotropic media, we have $E(\theta) = E$, $\mu(\theta) = \mu$ and $\nu(\theta) = \nu$ for all values of θ . For the sake of illustration, we consider one instance of each of the elastic symmetries introduced in this section and plot the corresponding generalized moduli on Figs. 1 through 5.

3 Green's functions for concentrated forces in a plane

A Green's function $G_{km} : \mathbb{R} \rightarrow \mathbb{R}$ is defined such that $G_{km} : \underline{x} \mapsto G_{km}(\underline{x})$ is the Cartesian component $u_k(\underline{x})$ of the displacement field of an infinitely large traction-free plane subjected to a concentrated force \underline{e}_m applied at the origin. First, we expect the Green's function to be such that the underlying linear elastic stress field satisfies equilibrium locally, namely

$$\partial_j [L_{ijkl} G_{km,l}(\underline{x})] = 0 \text{ for all } \underline{x} \text{ away from the origin.} \quad (5)$$

Equivalently, one can verify that every sub-domain of the plate containing the origin has a traction field on its boundary with a force resultant in equilibrium with the applied concentrated load. This can be expressed as follows:

$$\oint_{\mathcal{C}} L_{ijkl} G_{km,l}(\underline{x}) n_j(\underline{x}) ds + \delta_{im} = 0 \quad (6)$$

for all closed curves \mathcal{C} which contain the origin within their interior and where the concentrated load is denoted by \underline{e}_m . Second, it is sufficient that the stress field vanishes at all locations infinitely away from the origin for the traction-free condition to be satisfied. This is

$$\lim_{\|\underline{x}\| \rightarrow 0} L_{ijkl} G_{km,l}(\underline{x}) = 0. \quad (7)$$

Those conditions are used later to validate the Green's functions we obtain for different material symmetries.

4 2D Stroh formalism

The Stroh formalism rose from the work of Eshelby et al. (1953) who proposed a solution for the two-dimensional displacement fields due to dislocations in anisotropic media. The method was further developed and popularized by Stroh (1958, 1962), hence the reason for the term *Stroh formalism*. This goes as follows. First, without loss of generality, consider the following ansatz for the displacement field:

$$u_i(\underline{x}) = a_i f(z) \quad \text{where} \quad z = x_1 + px_2 \quad (8)$$

with p complex. Then, since

$$\partial_j[f^{(n)}(z)] = f^{(n+1)}(z)\partial_j[z] \quad (9)$$

$$= (\delta_{j1} + p\delta_{j2})f^{(n+1)}(z), \quad (10)$$

we have

$$u_{k,s}(\underline{x}) = \partial_s[a_k f(z)] = a_k f'(z)\partial_s[z] = (\delta_{s1} + p\delta_{s2})a_k f'(z) \quad (11)$$

and

$$u_{k,sj}(\underline{x}) = \partial_j[(\delta_{s1} + p\delta_{s2})a_k f'(z)] = (\delta_{s1} + p\delta_{s2})a_k \partial_j[f'(z)] = (\delta_{s1} + p\delta_{s2})a_k f''(z)\partial_j[z] \quad (12)$$

$$= (\delta_{j1} + p\delta_{j2})(\delta_{s1} + p\delta_{s2})a_k f''(z). \quad (13)$$

Local equilibrium is then stated as follows:

$$L_{ijks}u_{k,sj}(\underline{x}) = 0 \quad (14)$$

$$L_{ijks}(\delta_{j1} + p\delta_{j2})(\delta_{s1} + p\delta_{s2})a_k f''(z) = 0 \quad (15)$$

$$L_{ijks}(\delta_{j1} + p\delta_{j2})(\delta_{s1} + p\delta_{s2})a_k = 0 \quad (16)$$

$$[L_{i1k1} + p(L_{i1k2} + L_{i2k1}) + p^2 L_{i2k2}]a_k = 0 \quad (17)$$

which we may recast in

$$[Q_{ik} + p(R_{ik} + R_{ki}) + p^2 T_{ik}]a_k = 0 \quad (18)$$

where

$$Q_{ik} := L_{i1k1} \quad , \quad R_{ik} := L_{i1k2} \quad \text{and} \quad T_{ik} := L_{i2k2}. \quad (19)$$

Consequently, non-trivial solutions of the displacement field are zeros of the following characteristic equation:

$$P(p) := \sum_{k=0}^4 P_k p^k \quad (20)$$

where

$$P_0 = L_{1111}L_{1212} - L_{1112}L_{1112}, \quad (21)$$

$$P_1 = 2(L_{1111}L_{2212} - L_{1112}L_{1122}), \quad (22)$$

$$P_2 = L_{1111}L_{2222} + 2(L_{1112}L_{2212} - L_{1122}L_{1212}) - L_{1122}L_{1122}, \quad (23)$$

$$P_3 = 2(L_{1112}L_{2222} - L_{1122}L_{2212}), \quad (24)$$

$$P_4 = L_{1212}L_{2222} - L_{2212}L_{2212}. \quad (25)$$

The roots of the characteristic equation form the Stroh eigensystem given by

$$\{(p_\alpha, \bar{p}_\alpha, \underline{a}^\alpha, \bar{\underline{a}}^\alpha) \mid P(p_\alpha) = 0, \Im\{p_\alpha\} > 0, \alpha = 1, 2\} \quad (26)$$

for which the Stroh eigenvectors \underline{a}^α satisfy

$$[L_{i1k1} + p_\alpha(L_{i1k2} + L_{i2k1}) + p_\alpha^2 L_{i2k2}]a_k^\alpha = 0. \quad (27)$$

For non-degenerate symmetries, *i.e.* with independent Stroh eigenvectors \underline{a}^α , complete solutions of the displacement field take the form

$$\underline{u}(\underline{x}) = \underline{a}^1 f_1(z_1) + \underline{a}^1 f_3(\bar{z}_1) + \underline{a}^2 f_2(z_2) + \underline{a}^2 f_4(\bar{z}_2) \quad (28)$$

where f_α are arbitrary functions that depend on the applied boundary conditions. Note that $z_\alpha := x_1 + p_\alpha x_2$. By linear elasticity, we then have

$$\sigma_{i1} = (Q_{ik} + pR_{ik})a_k f'(z) \quad \text{and} \quad \sigma_{i2} = (R_{ki} + pT_{ik})a_k f'(z). \quad (29)$$

But, since local equilibrium requires $Q_{ik} + p(R_{ik} + R_{ki}) + p^2 T_{ik} = 0$, we have

$$R_{ki} + pT_{ik} = -\frac{1}{p}(Q_{ik} + pR_{ik}). \quad (30)$$

The expressions for the stress components then become

$$\begin{aligned} \sigma_{i1} &= (Q_{ik} + pR_{ik})a_k f' \\ &= -p(R_{ki} + pT_{ik})a_k f'(z) \end{aligned} \quad \text{and} \quad \begin{aligned} \sigma_{i2} &= (R_{ki} + pT_{ik})a_k f'(z) \\ &= -(1/p)(Q_{ik} + pR_{ik})a_k f'(z) \end{aligned} \quad (31)$$

which we recast in

$$\sigma_{i1} = -pb_i f'(z), \quad \sigma_{i2} = b_i f'(z) \quad (32)$$

with

$$\begin{aligned} b_i &:= (R_{ki} + pT_{ik})a_k \\ &= -\frac{1}{p}(Q_{ik} + pR_{ik})a_k. \end{aligned}$$

Therefore, we can appropriately define the following stress function $\varphi_i(z) = b_i f(z)$ such that

$$\varphi_{i,j}(z) = b_i(\delta_{j1} + p\delta_{j2})f'(z), \quad (33)$$

which implies

$$\begin{aligned} \varphi_{i,1}(z) &= b_i f'(z) = \sigma_{i2}(z), \\ \varphi_{i,2}(z) &= pb_i f'(z) = -\sigma_{i1}(z). \end{aligned}$$

Then, by symmetry of the Cauchy stress tensor, we have

$$\begin{aligned} \varphi_{1,1} + \varphi_{2,2} &= 0 \\ (b_1 + pb_2)f'(z) &= 0 \\ b_1 + pb_2 &= 0. \end{aligned}$$

Under the assumption of non-degeneracy, *i.e.* linearly independent $\underline{a}^1, \underline{a}^1, \underline{a}^2$ and \underline{a}^2 , an ansatz for the complete stress function is given by the following superposition:

$$\underline{\varphi}(\underline{x}) = \underline{b}^1 f_1(z_1) + \underline{b}^1 f_3(\bar{z}_1) + \underline{b}^2 f_2(z_2) + \underline{b}^2 f_4(\bar{z}_2). \quad (34)$$

More particularly, solutions with the property

$$f_1(z_1) = q_1 f(z_1), \quad f_2(z_2) = q_2 f(z_2), \quad f_3(\bar{z}_1) = \bar{q}_1 \bar{f}(\bar{z}_1), \quad f_4(\bar{z}_2) = \bar{q}_2 \bar{f}(\bar{z}_2) \quad (35)$$

are usually considered. Then, since

$$2\Re\{\underline{a}^\alpha q_\alpha f(z_\alpha)\} = \underline{a}^\alpha q_\alpha f(z_\alpha) + \underline{a}^\alpha \bar{q}_\alpha \bar{f}(\bar{z}_\alpha) \quad \text{and} \quad 2\Re\{\underline{b}^\alpha q_\alpha f(z_\alpha)\} = \underline{b}^\alpha q_\alpha f(z_\alpha) + \underline{b}^\alpha \bar{q}_\alpha \bar{f}(\bar{z}_\alpha), \quad (36)$$

we have

$$\underline{u}(\underline{x}) = 2\Re\{\underline{a}^1 f(z_1)q_1 + \underline{a}^2 f(z_2)q_2\} \quad \text{and} \quad \underline{\varphi}(\underline{x}) = 2\Re\{\underline{b}^1 f(z_1)q_1 + \underline{b}^2 f(z_2)q_2\} \quad (37)$$

so that if q_α is replaced by $-iq_\alpha$, $\Re\{-iz\} = \Im\{z\}$ implies

$$\begin{aligned} \underline{u}(\underline{x}) &= 2\Im\{\underline{a}^1 f(z_1)q_1 + \underline{a}^2 f(z_2)q_2\}, \\ \underline{\varphi}(\underline{x}) &= 2\Im\{\underline{b}^1 f(z_1)q_1 + \underline{b}^2 f(z_2)q_2\} \end{aligned}$$

in which one has to solve for $f(z)$, q_1 and q_2 to satisfy specific boundary conditions.

4.1 Concentrated force applied at the origin

A more particular expression of the displacement field is obtained after specifying the boundary conditions. If a concentrated force \underline{f} is applied within the plane, every closed curve \mathcal{C} whose interior contains the point of application of the force should be such that

$$\oint_{\mathcal{C}} \sigma_{ij}(\underline{x}) n_j(\underline{x}) ds + f_i = 0.$$

Note that from the definition of the stress function, we have $\sigma_{i1} = -\varphi_{i,2}$ and $\sigma_{i2} = \varphi_{i,1}$. Meanwhile, the exterior normal to the curve with arc length s has components $n_1 = -\partial x_2 / \partial s$ and $n_2 = \partial x_1 / \partial s$ such that

$$\sigma_{ij}(\underline{x}) n_j(\underline{x}) = \varphi_{i,j}(\underline{x}) \frac{\partial x_j}{\partial s} = \frac{d\varphi_i(\underline{x})}{ds} \quad (38)$$

and

$$\oint_{\mathcal{C}} \sigma_{ij}(\underline{x}) n_j(\underline{x}) ds = \oint_{\mathcal{C}} \frac{d\varphi_i(\underline{x})}{ds} ds = \varphi_i(s_b) - \varphi_i(s_a).$$

We then have

$$\varphi_i(\ell) - \varphi_i(0) + f_i = 0$$

where ℓ is the length of the curve.

From now on, we redefine q_α such that

$$\underline{u}(\underline{x}) = \frac{1}{\pi} \Im \{ \underline{a}^1 f(z_1) q_1^\infty + \underline{a}^2 f(z_2) q_2^\infty \} \quad \text{and} \quad \underline{\varphi}(\underline{x}) = \frac{1}{\pi} \Im \{ \underline{b}^1 f(z_1) q_1^\infty + \underline{b}^2 f(z_2) q_2^\infty \}. \quad (39)$$

Also, we consider an ansatz of the form $f(z_\alpha) = \ln(z_\alpha)$. As we let $x_1 = r \cos \theta$ and $x_2 = r \sin \theta$, it is clear that away from the origin (for $r > 0$), we have

$$\ln(z) = \begin{cases} \ln(r) & \text{if } \theta = 0, \\ \ln(r) \pm i\pi & \text{if } \theta = \pm\pi \end{cases} \quad (40)$$

which implies

$$\ln(z)|_{\theta=\pi} - \ln(z)|_{\theta=-\pi} = 2\pi i. \quad (41)$$

Consequently, we have

$$\sum_{\alpha=1}^2 \underline{b}^\alpha q_\alpha^\infty [f(z_\alpha)|_{\theta=\pi} - f(z_\alpha)|_{\theta=-\pi}] = 2\pi i (\underline{b}^1 q_1^\infty + \underline{b}^2 q_2^\infty) \quad (42)$$

and

$$\Im \left(\sum_{\alpha=1}^2 \underline{b}^\alpha q_\alpha^\infty [f(z_\alpha)|_{\theta=\pi} - f(z_\alpha)|_{\theta=-\pi}] \right) = 2\pi \Re \{ \underline{b}^1 q_1^\infty + \underline{b}^2 q_2^\infty \}. \quad (43)$$

Then, for equilibrium to be satisfied, we must have

$$\underline{\varphi}(r, \pi) - \underline{\varphi}(r, -\pi) = \underline{f} \implies 2\Re \{ \underline{b}^1 q_1^\infty + \underline{b}^2 q_2^\infty \} = \underline{f} \implies \sum_{\alpha=1}^2 \left(\underline{b}^\alpha q_\alpha^\infty + \overline{\underline{b}}^\alpha \overline{q_\alpha^\infty} \right) = \underline{f}. \quad (44)$$

By compatibility of the displacement field, we also have

$$\underline{u}(r, \pi) - \underline{u}(r, -\pi) = \underline{0} \implies 2\Re \{ \underline{a}^1 q_1^\infty + \underline{a}^2 q_2^\infty \} = \underline{0} \implies \sum_{\alpha=1}^2 (\underline{a}^\alpha q_\alpha^\infty + \overline{\underline{a}}^\alpha \overline{q_\alpha^\infty}) = \underline{0} \quad (45)$$

For non-degenerate media, the Stroh eigenvectors have the following properties

$$\underline{a}^\alpha \cdot \underline{b}^\beta + \underline{a}^\beta \cdot \underline{b}^\alpha = \delta_{\alpha\beta} = \overline{\underline{a}}^\alpha \cdot \overline{\underline{b}}^\beta + \overline{\underline{a}}^\beta \cdot \overline{\underline{b}}^\alpha \quad (46)$$

and

$$\underline{a}^\alpha \cdot \overline{\underline{b}}^\beta + \overline{\underline{a}}^\beta \cdot \underline{b}^\alpha = 0 = \overline{\underline{a}}^\alpha \cdot \underline{b}^\beta + \underline{a}^\beta \cdot \overline{\underline{b}}^\alpha \quad (47)$$

which we refer to as the orthogonality condition (Ting, 1996). Consequently, we can solve for q_α^∞ and \bar{q}_α^∞ in Eq. (44) and (45). We obtain

$$q_\alpha^\infty = \underline{a}^\alpha \cdot \underline{f} \quad \text{and} \quad \bar{q}_\alpha^\infty = \bar{\underline{a}}^\alpha \cdot \underline{f} \quad (48)$$

so that we have

$$\underline{u}(\underline{x}) = \frac{1}{\pi} \Im \{ \underline{a}^1 \otimes \underline{a}^1 \ln(z_1) + \underline{a}^2 \otimes \underline{a}^2 \ln(z_2) \} \cdot \underline{f}. \quad (49)$$

Let \underline{f} be a concentrated force \underline{e}_m so that the following expression for the Green's function is obtained,

$$G_{km}(\underline{x}) = \frac{1}{\pi} \Im \{ a_k^1 a_m^1 \ln(z_1) + a_k^2 a_m^2 \ln(z_2) \} \quad (50)$$

which, once again, is complete only if $\underline{a}^1, \bar{\underline{a}}^1, \underline{a}^2$ and $\bar{\underline{a}}^2$ are linearly independent.

5 2D Barnett-Lothe integral formalism

The displacement field and corresponding Green's function obtained by the Stroh formalism, see Eqs. (49) and (50) are valid only if the Stroh eigenvectors are independent. Otherwise, the medium is referred to as degenerate and the solution is incomplete. Different approaches can be used to complete the solution, see Ting (1996) for more details. Instead, we find it more convenient to resort to the Barnett-Lothe integral formalism (Barnett and Lothe, 1973) which proposes a solution for the displacement field that circumvent both those difficulties encountered for degenerate media and, the need to solve for the Stroh eigenvalue problem. The solution obtained by the authors is

$$2\underline{u}(r, \theta) = -\frac{1}{\pi} \ln(r) \mathbf{H} \cdot \underline{f} - \mathbf{S}(\theta) \cdot \mathbf{H} \cdot \underline{f} - \mathbf{H}(\theta) \cdot \mathbf{S}^T \cdot \underline{f} \quad (51)$$

where

$$\mathbf{S}(\theta) = \frac{1}{\pi} \int_0^\theta \mathbf{N}^1(\psi) d\psi \quad \text{and} \quad \mathbf{H}(\theta) = \frac{1}{\pi} \int_0^\theta \mathbf{N}^2(\psi) d\psi \quad (52)$$

are referred to as the first and second incomplete Barnett-Lothe integrals with $\mathbf{S} := \mathbf{S}(\pi)$ and $\mathbf{H} := \mathbf{H}(\pi)$ being their complete counterparts for which the *Barnett-Lothe integrands* are

$$\mathbf{N}^1(\theta) = -\tilde{\mathbf{T}}^{-1}(\theta) \cdot \tilde{\mathbf{R}}^T(\theta) \quad \text{and} \quad \mathbf{N}^2(\theta) = \tilde{\mathbf{T}}^{-1}(\theta) \quad (53)$$

with

$$\tilde{R}_{ik}(\theta) := L_{ijkl} n_j(\theta) m_l(\theta) \quad \text{and} \quad \tilde{T}_{ik}(\theta) := L_{ijkl} m_j(\theta) m_l(\theta) \quad (54)$$

where \underline{n} is a unit vector and \underline{m} is its active $\pi/2$ counter-clockwise rotation. Let them be $\underline{n}(\theta) = \cos(\theta)\underline{e}_1 + \sin(\theta)\underline{e}_2$ and $\underline{m}(\theta) = -\sin(\theta)\underline{e}_1 + \cos(\theta)\underline{e}_2$. Then, we have

$$\begin{aligned} \tilde{R}_{ik}(\theta) &= L_{i1k2} \cos^2(\theta) + (L_{i2k2} - L_{i1k1}) \cos(\theta) \sin(\theta) - L_{i2k1} \sin^2(\theta), \\ \tilde{T}_{ik}(\theta) &= L_{i2k2} \cos^2(\theta) - (L_{i1k2} + L_{i2k1}^0) \cos(\theta) \sin(\theta) + L_{i1k1} \sin^2(\theta). \end{aligned}$$

Note that, in general, we have

$$N_{ji}^1(\theta) \neq N_{ij}^1(\theta) \quad \text{and} \quad N_{ji}^2(\theta) = N_{ij}^2(\theta)$$

which implies $\mathbf{H}^T = \mathbf{H}$. Eventually, similarly as before, we let \underline{f} be a concentrated force \underline{e}_m and we obtain the following expression for the Green's function:

$$-2G_{km}(r, \theta) = (\pi)^{-1} \ln(r) H_{km} + S_{ks}(\theta) H_{sm} + H_{ks}(\theta) S_{ms}. \quad (55)$$

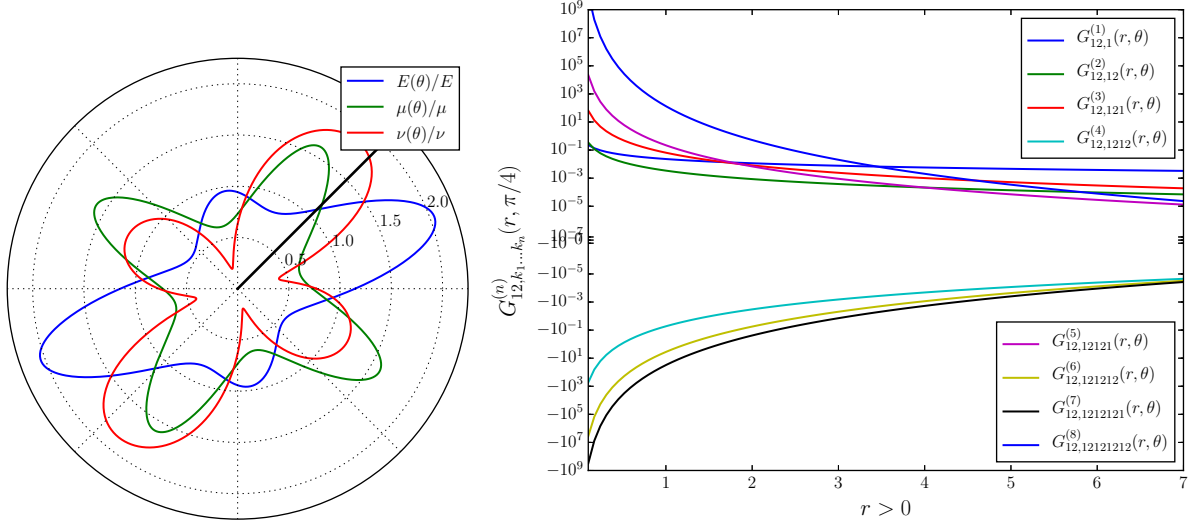


Figure 1: Polar diagram of generalized moduli of an anisotropic plane (on the left) and some components of gradients of the Green's function (on the right) computed along the black of the polar diagram.

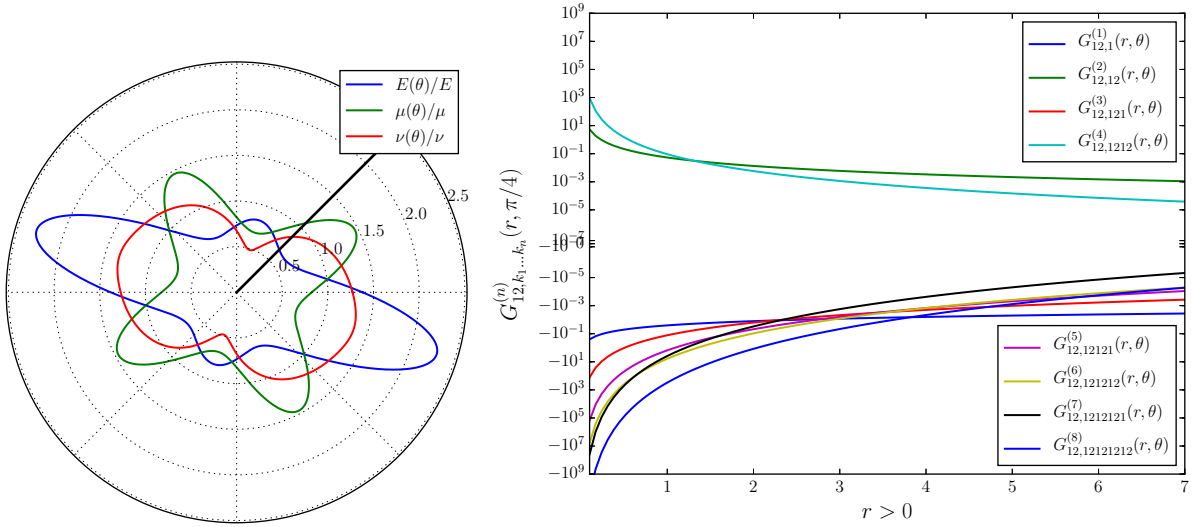


Figure 2: Polar diagram of generalized moduli of an orthotropic plane (on the left) and some components of gradients of the Green's function (on the right) computed along the black of the polar diagram.

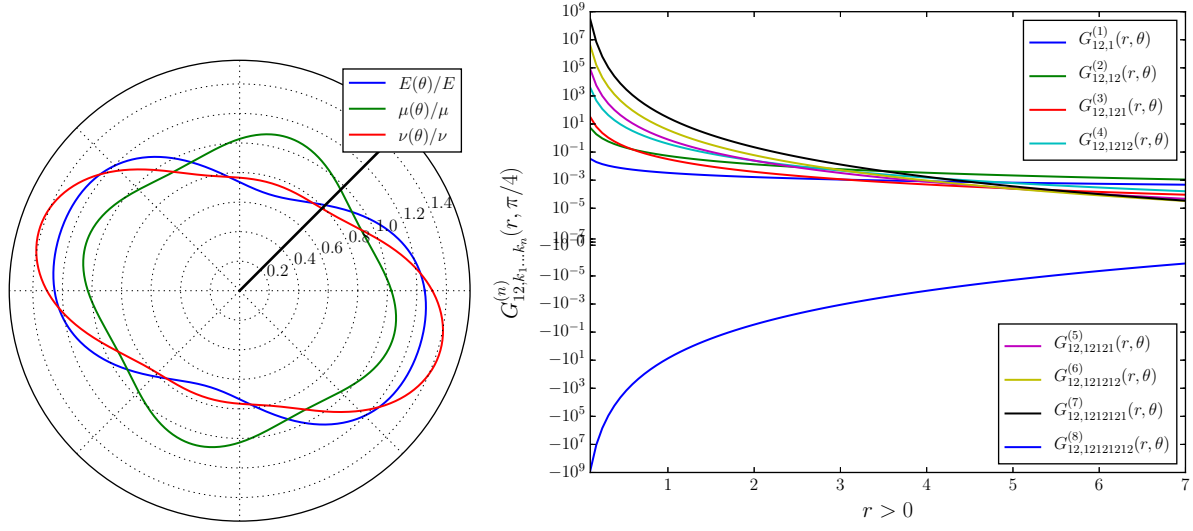


Figure 3: Polar diagram of generalized moduli of a R0-orthotropic plane (on the left) and some components of gradients of the Green's function (on the right) computed along the black of the polar diagram.

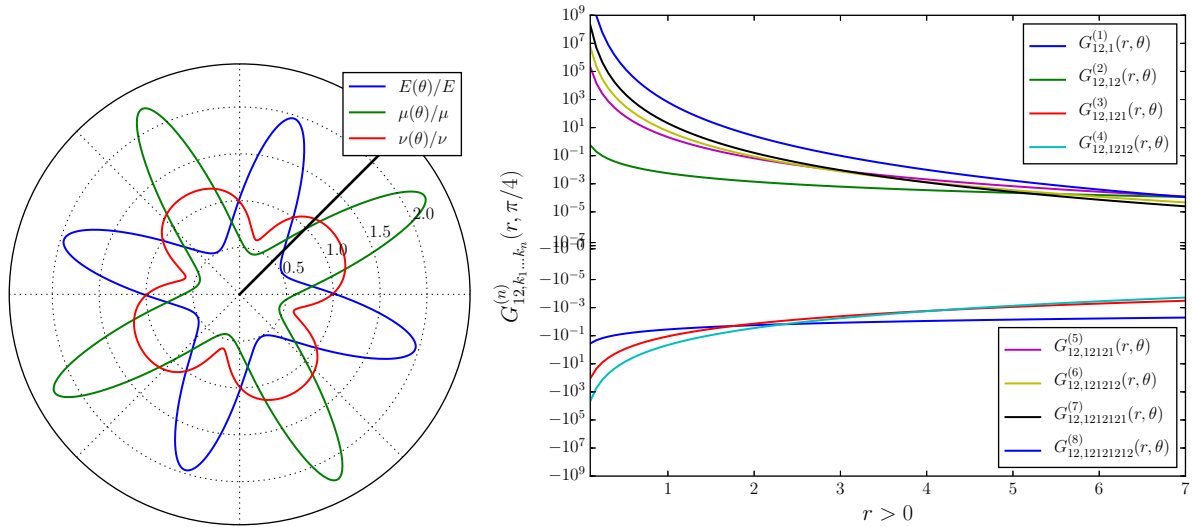


Figure 4: Polar diagram of generalized moduli of a square symmetric plane (on the left) and some components of gradients of the Green's function (on the right) computed along the black of the polar diagram.

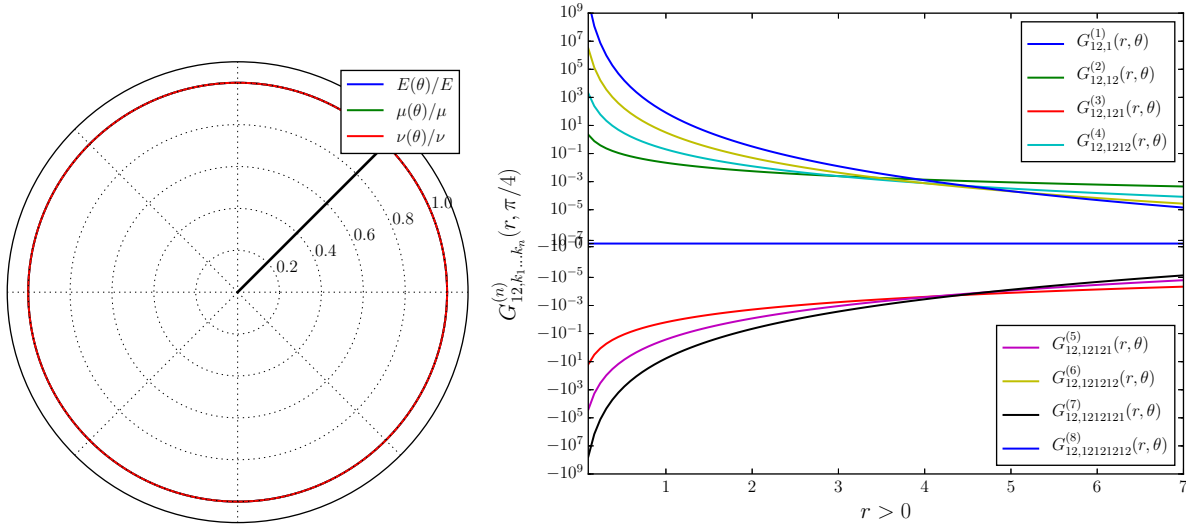


Figure 5: Polar diagram of generalized moduli of an isotropic plane (on the left) and some components of gradients of the Green's function (on the right) computed along the black of the polar diagram.

6 Recursive expressions for the gradients of the Green's function

From now on, we assume the Green's functions of interest have a form as given by Eq. (55). Then, we are interested in the form taken by its gradients. First, let \tilde{f} be a function of \underline{x} and let $\underline{x} = r\underline{n}$ with $r \geq 0$ and $\|\underline{n}\| = 1$. Then, we can write $n_1(\theta) = \cos(\theta)$ and $n_2(\theta) = \sin(\theta)$ where θ is the counter-clockwise positive between \underline{e}_1 and \underline{x} . Consequently, we have

$$\partial_{k_1} \tilde{f}(r, \theta) = n_{k_1}(\theta) \partial_r f(r, \theta) + r^{-1} m_{k_1}(\theta) \partial_\theta f(r, \theta)$$

where \underline{m} is the active $\pi/2$ counter-clockwise rotation of \underline{n} , namely $\underline{m}(\theta) = -\sin(\theta)\underline{e}_1 + \cos(\theta)\underline{e}_2$. Once applied to our expression of the Green's function, this gives

$$2G_{ij,k_1}^{(1)}(r, \theta) = -\frac{r^{-1}}{\pi} H_{ij} n_{k_1}(\theta) - r^{-1} \partial_\theta [S_{is}(\theta)] H_{sj} m_{k_1}(\theta) - r^{-1} \partial_\theta [H_{is}(\theta)] S_{js} m_{k_1}(\theta) \quad (56)$$

in which we differentiate the Barnett-Lothe integrals as follows,

$$\begin{aligned} \pi \partial_\theta [S_{ij}(\theta)] &= N_{ij}^1(\theta), \\ \pi \partial_\theta [H_{ij}(\theta)] &= N_{ij}^2(\theta), \end{aligned}$$

so that we obtain

$$2G_{ij,k_1}^{(1)}(r, \theta) = -\frac{r^{-1}}{\pi} [H_{ij} n_{k_1}(\theta) + N_{is}^1(\theta) H_{sj} m_{k_1}(\theta) + N_{is}^2(\theta) S_{js} m_{k_1}(\theta)] \quad (57)$$

which we recast in

$$2G_{ij,k_1}^{(1)}(r, \theta) = g^1(r) h_{ijk_1}^1(\theta) \quad (58)$$

where

$$h_{ijk_1}^1(\theta) := H_{ij} n_{k_1}(\theta) + N_{is}^1(\theta) H_{sj} m_{k_1}(\theta) + N_{is}^2(\theta) S_{js} m_{k_1}(\theta), \quad (59)$$

$$g^1(r) := -\frac{r^{-1}}{\pi}. \quad (60)$$

Similarly, as we have

$$\begin{aligned} \partial_{k_2} [g^1(r) h_{ijk_1}^1(\theta)] &= n_{k_2}(\theta) \partial_r [g^1(r)] h_{ijk_1}^1(\theta) + r^{-1} m_{k_2}(\theta) g^1(r) \partial_\theta [h_{ijk_1}^1(\theta)] \\ \partial_{k_2} [g^1(r) h_{ijk_1}^1(\theta)] &= n_{k_2}(\theta) \pi^{-1} r^{-2} h_{ijk_1}^1(\theta) - r^{-1} m_{k_2}(\theta) \pi^{-1} r^{-1} \partial_\theta [h_{ijk_1}^1(\theta)] \\ \partial_{k_2} [g^1(r) h_{ijk_1}^1(\theta)] &= \frac{r^{-2}}{\pi} [h_{ijk_1}^1(\theta) n_{k_2}(\theta) - \partial_\theta [h_{ijk_1}^1(\theta)] m_{k_2}(\theta)], \end{aligned}$$

we get

$$2G_{ij,k_1k_2}^{(2)}(r, \theta) = g^2(r)h_{ij,k_1k_2}^2(\theta) \quad (61)$$

in which we have

$$g^2(r) := \frac{r^{-2}}{\pi} \quad (62)$$

$$h_{ij,k_1k_2}^2(\theta) := h_{ij,k_1}^1(\theta)n_{k_2}(\theta) - \partial_\theta[h_{ij,k_1}^1(\theta)]m_{k_2}(\theta). \quad (63)$$

Once again, we proceed similarly and get

$$\begin{aligned} \partial_{k_3}[g^2(r)h_{ij,k_1k_2}^2(\theta)] &= n_{k_3}(\theta)\partial_r[g^2(r)]h_{ij,k_1k_2}^2(\theta) + r^{-1}m_{k_3}(\theta)g^2(r)\partial_\theta[h_{ij,k_1k_2}^2(\theta)] \\ \partial_{k_3}[g^2(r)h_{ij,k_1k_2}^2(\theta)] &= -2n_{k_3}(\theta)\pi^{-1}r^{-3}h_{ij,k_1k_2}^2(\theta) + r^{-1}m_{k_3}(\theta)\pi^{-1}r^{-2}\partial_\theta[h_{ij,k_1k_2}^2(\theta)] \\ \partial_{k_3}[g^2(r)h_{ij,k_1k_2}^2(\theta)] &= -\frac{r^{-3}}{\pi}[n_{k_3}(\theta)h_{ij,k_1k_2}^2(\theta) - m_{k_3}(\theta)\partial_\theta[h_{ij,k_1k_2}^2(\theta)]] \end{aligned}$$

so that

$$2G_{ij,k_1k_2k_3}^{(3)}(r, \theta) = g^3(r)h_{ij,k_1k_2k_3}^3(\theta)$$

where

$$\begin{aligned} g^3(r) &:= -\frac{r^{-3}}{\pi} \\ h_{ij,k_1k_2k_3}^3(\theta) &:= h_{ij,k_1k_2}^2(\theta)n_{k_3}(\theta) - \partial_\theta[h_{ij,k_1k_2}^2(\theta)]m_{k_3}(\theta). \end{aligned}$$

Eventually, we find that

$$2\pi G_{ij,k_1\dots k_n}^{(n)}(r, \theta) = (-r)^{-n} \left[h_{ij,k_1\dots k_{n-1}}^{n-1}(\theta)n_{k_n}(\theta) - \partial_\theta[h_{ij,k_1\dots k_{n-1}}^{n-1}(\theta)]m_{k_n}(\theta) \right] \quad (64)$$

where

$$h_{ij,k_1}^1(\theta) = H_{ij}n_{k_1}(\theta) + [N_{is}^1(\theta)H_{sj} + N_{is}^2(\theta)S_{js}]m_{k_1}(\theta) \quad (65)$$

and

$$h_{ij,k_1\dots k_n}^n(\theta) = h_{ij,k_1\dots k_{n-1}}^{n-1}(\theta)n_{k_n}(\theta) - \partial_\theta[h_{ij,k_1\dots k_{n-1}}^{n-1}(\theta)]m_{k_n}(\theta) \quad (66)$$

in which we have

$$\partial_\theta^k[h_{ij,k_1\dots k_n}^n(\theta)] = \sum_{s=0}^{k+1} \binom{k+1}{s} \partial_\theta^s[h_{ij,k_1\dots k_{n-1}}^{n-1}(\theta)]\partial_\theta^{k-s}[n_{k_n}] \quad (67)$$

and

$$\partial_\theta^k[h_{ij,k_1}^1(\theta)] = H_{ij}\partial_\theta^k[n_{k_1}(\theta)] + \sum_{s=0}^k \binom{k}{s} \{H_{lj}\partial_\theta^{k-s}[N_{il}^1(\theta)] + S_{jl}\partial_\theta^{k-s}[N_{il}^2(\theta)]\} \partial_\theta^s[m_{k_1}(\theta)]. \quad (68)$$

Note that we also have

$$\partial_\theta^k[n_{k_1}(\theta)] = (-1)^{\frac{k(k+3)}{2}}[n_{k_1}(\theta)]^{\frac{(-1)^{k+1}}{2}}[m_{k_1}(\theta)]^{\frac{(-1)^{k+1}+1}{2}} \quad (\text{no sum over } k_1), \quad (69)$$

$$\partial_\theta^k[m_{k_1}(\theta)] = (-1)^{\frac{(k+1)(k+4)}{2}}[n_{k_1}(\theta)]^{\frac{(-1)^{k+1}+1}{2}}[m_{k_1}(\theta)]^{\frac{(-1)^{k+2}+1}{2}} \quad (\text{no sum over } k_1). \quad (70)$$

A recursive algorithm can easily be developed using Eqs. (64)–(70) to compute the gradients of arbitrary order of the Green's function. Our implementation of this algorithm can be found in `dG_recursive.cpp`. The Barnett-Lothe integrands, and their derivatives, which take different forms depending on the material symmetry of interest, are derived analytically up

to the seventh order. Although those derivations are straightforward, the resulting expressions are rather cumbersome; see in the following files,

```
dkN1_anisotropic.cpp, dkN2_anisotropic.cpp,
dkN1_orthotropic.cpp, dkN2_orthotropic.cpp,
dkN1_r0_orthotropic.cpp, dkN2_r0_orthotropic.cpp,
dkN1_square_symmetric.cpp, dkN2_square_symmetric.cpp,
dkN1_isotropic.cpp, dkN2_isotropic.cpp,
```

for the first and second integrands, respectively. Some components of the gradients of the Green's functions of the media presented before are computed up to the eighth order. The components are computed along the black line displayed on the corresponding polar diagrams, see Figs. 1 through 5.

7 Symmetry-dependent results

7.1 Orthotropies

For both "regular" orthotropic and R0-orthotropic media, we find that $\text{tr}\mathbf{S} = 0$, which implies $S_{11} = -S_{22}$ stands for all coordinate frames. Consequently, the Reynolds glyph of \mathbf{S} has a vanishing pole which, equivalently, means that one of the principal components of the tensor is zero.

7.2 Square symmetry

For square symmetric media, we find that $S_{11} = S_{22} = 0$ for all coordinate frames. Also, we find $S_{12} = -S_{21}$ so that \mathbf{S} is antisymmetric. We also have $H_{11} = H_{22}$.

7.3 Isotropy

For isotropic media, the components of the first complete Barnett-Lothe integral are

$$\begin{aligned} S_{11} &= S_{22} = 0 \\ S_{12} &= -\frac{\mu}{\kappa + \mu} \\ S_{21} &= -S_{12} \end{aligned}$$

while those of the second complete Barnett-Lothe integral are

$$\begin{aligned} H_{11} &= \frac{\kappa + 2\mu}{2\mu(\kappa + \mu)} \\ H_{22} &= \frac{\kappa + 2\mu}{2\mu(\kappa + \mu)} \\ H_{12} &= H_{21} = 0. \end{aligned}$$

Consequently, we have that \mathbf{S} is antisymmetric while \mathbf{H} is isotropic. The Barnett-Lothe integrands also take simple forms

$$\begin{aligned} N_{11}^1(\theta) &= \frac{\kappa \sin(2\theta)}{\kappa + \mu} \\ N_{22}^1(\theta) &= -N_{11}^1(\theta) \\ N_{12}^1(\theta) &= -\frac{\mu + \kappa \cos(2\theta)}{\kappa + \mu} \\ N_{21}^1(\theta) &= \frac{\mu - \kappa \cos(2\theta)}{\kappa + \mu} \end{aligned}$$

and

$$N_{11}^2(\theta) = \frac{2\mu + \kappa[1 + \cos(2\theta)]}{2\mu(\kappa + \mu)}$$

$$N_{22}^2(\theta) = \frac{2\mu + \kappa[1 - \cos(2\theta)]}{2\mu(\kappa + \mu)}$$

$$N_{12}^2(\theta) = N_{21}^2(\theta) = \frac{\kappa \sin(2\theta)}{2\mu(\kappa + \mu)}.$$

We then have the following expressions for their derivatives,

$$\begin{aligned}\partial_\theta^k[N_{11}^1(\theta)] &= \frac{2^k \kappa}{\kappa + \mu} \sin\left(\frac{k\pi}{2} + 2\theta\right) \\ \partial_\theta^k[N_{22}^1(\theta)] &= -\partial_\theta^k[N_{11}^1(\theta)] \\ \partial_\theta^k[N_{12}^1(\theta)] &= -\frac{2^k \kappa}{\kappa + \mu} \cos\left(\frac{k\pi}{2} + 2\theta\right) \quad (\text{for } k \geq 1) \\ \partial_\theta^k[N_{21}^1(\theta)] &= \partial_\theta^k[N_{12}^1(\theta)] \quad (\text{for } k \geq 1)\end{aligned}$$

and

$$\begin{aligned}\partial_\theta^k[N_{11}^2(\theta)] &= \frac{2^{k-1} \kappa}{\mu(\kappa + \mu)} \cos\left(\frac{k\pi}{2} + 2\theta\right) \quad (\text{for } k \geq 1) \\ \partial_\theta^k[N_{22}^2(\theta)] &= -\partial_\theta^k[N_{11}^2(\theta)] \quad (\text{for } k \geq 1) \\ \partial_\theta^k[N_{12}^2(\theta)] &= \partial_\theta^k[N_{21}^2(\theta)] = \frac{2^{k-1} \kappa}{\mu(\kappa + \mu)} \sin\left(\frac{k\pi}{2} + 2\theta\right).\end{aligned}$$

for the second integrands. We also use the recursive algorithm to compute the gradients of the Green's function of isotropic media.

8 Verification and validation

The method proposed is validated under the following conditions. First, the expressions obtained for the Green's functions are, for every symmetry of interest, such that the local statement of equilibrium is satisfied. Second, the underlying stress field has vanishing components at all locations infinitely remote from the origin. Third, the traction field on every arbitrary closed curve in the plane with the origin in its interior is in equilibrium with the prescribed concentrated force. Fourth, the expressions for the gradients obtained through the recursive approach are the same as the ones obtained by straightforward differentiation of the Green's functions, assuming the complete Barnett-Lothe integrals are known.

The first, second and fourth conditions of the validation process are carried over analytically, for each symmetry of interest, using Mathematica, see supporting file **GreenAnisotropic2D.wl** for more details. The third condition is carried over numerically making use of the code implemented. In what follows, we briefly describe how this condition is verified.

8.1 Global equilibrium

For every sub-domain of the plane containing the origin, we want to verify that the traction field on its boundary is in equilibrium with an applied concentrated load \underline{e}_m . Obviously, it is not practically possible to make such a verification for all closed curves containing the origin. Nevertheless, we can do for some random closed curves.

8.1.1 Random curves

Let the random closed curve $\underline{\alpha} : \theta \mapsto r(\theta)[\cos(\theta)\underline{e}_1 + \sin(\theta)\underline{e}_2]$ be specified by

$$r(\theta) = 1 + \frac{1}{n} \sum_{k=0}^{n-1} A_k \cos(k\theta) \quad (71)$$

where $A_k \sim \mathcal{U}(-2/5, 2/5)$ are independently and identically distributed random variables. A non-normalized counter-clockwise tangent vector to the curve is then given by

$$\begin{aligned}\partial_\theta[\underline{\alpha}(\theta)] &= -\left\{ \sin(\theta) + \frac{1}{n} \sum_{k=0}^{n-1} A_k [k \sin(k\theta) \cos(\theta) + \cos(k\theta) \sin(\theta)] \right\} \underline{e}_1 \\ &\quad + \left\{ \cos(\theta) + \frac{1}{n} \sum_{k=0}^{n-1} A_k [\cos(k\theta) \cos(\theta) - k \sin(k\theta) \sin(\theta)] \right\} \underline{e}_2\end{aligned} \quad (72)$$

which has magnitude

$$\|\partial_\theta[\underline{\alpha}(\theta)]\| = \sqrt{1 + \frac{2}{n} \sum_{k=0}^{n-1} A_k \cos(k\theta) + \left[\frac{1}{n} \sum_{k=0}^{n-1} A_k \cos(k\theta) \right]^2 + \left[\frac{1}{n} \sum_{k=0}^{n-1} k A_k \sin(k\theta) \right]^2}. \quad (73)$$

A non-normalized outward normal vector to the curve is then given by

$$\underline{n}(\theta) = \frac{\partial_\theta[\underline{\alpha}(\theta)]}{\|\partial_\theta[\underline{\alpha}(\theta)]\|} \cdot (\underline{e}_2 \otimes \underline{e}_1 - \underline{e}_1 \otimes \underline{e}_2). \quad (74)$$

8.1.2 Traction integration

The traction equilibrium is stated as follows,

$$\oint_C L_{ijkl} G_{km,l}(\underline{x}) n_j(\underline{x}) ds + \delta_{im} = 0, \quad (75)$$

so that we need to compute the integral

$$\oint_C L_{ijkl} G_{km,l}(\underline{x}) n_j(\underline{x}) ds \quad (76)$$

where the arc-length increment ds is $\|\partial_\theta[\underline{\alpha}(\theta)]\| d\theta$ so that we want to verify

$$\int_{\theta=0}^{2\pi} L_{ijkl} G_{km,l}(r(\theta), \theta) n_j(\theta) \|\partial_\theta[\underline{\alpha}(\theta)]\| d\theta + \delta_{im} = 0. \quad (77)$$

This integral is implemented and done numerically for different material instances. For the sake of illustration, we plot some the traction fields on random curves which, we find, are equilibrated with concentrated unit loads applied at the origin. See Figs. Fig. 6 through 10.

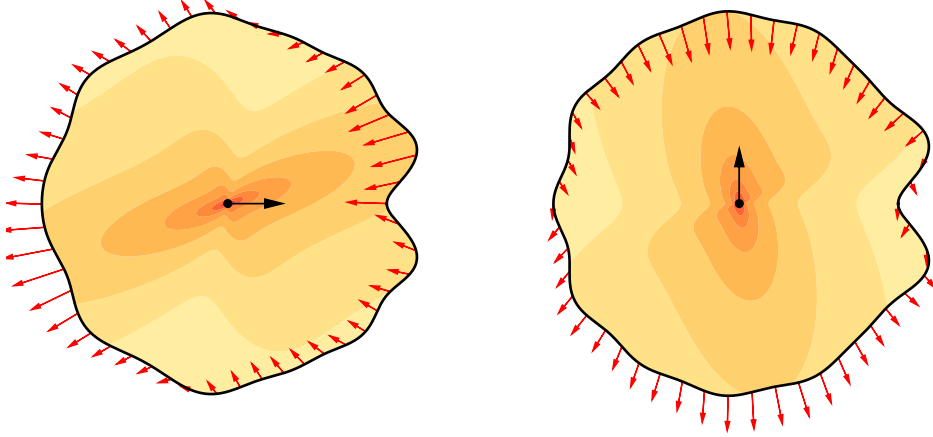


Figure 6: Equilibrated traction fields on random curves in an anisotropic plane subjected to a concentrated force \underline{e}_1 (on the left) and \underline{e}_2 (on the right).

8.2 Verification

We consider the validation of equilibrium through numerical computation of the traction field on random curves as a verification of our implementation. Another verification of the implementation/installation is done. For each material symmetry of interest, several "medium" instances are drawn. Several components of the gradients of different orders of the underlying Green's functions are evaluated at some specific locations using Mathematica. Those values are stored and used as references for comparison with the values computed using the Python library. Both implementation verification tasks are carried over by launching the script `test.py` after compilation of the Python library.

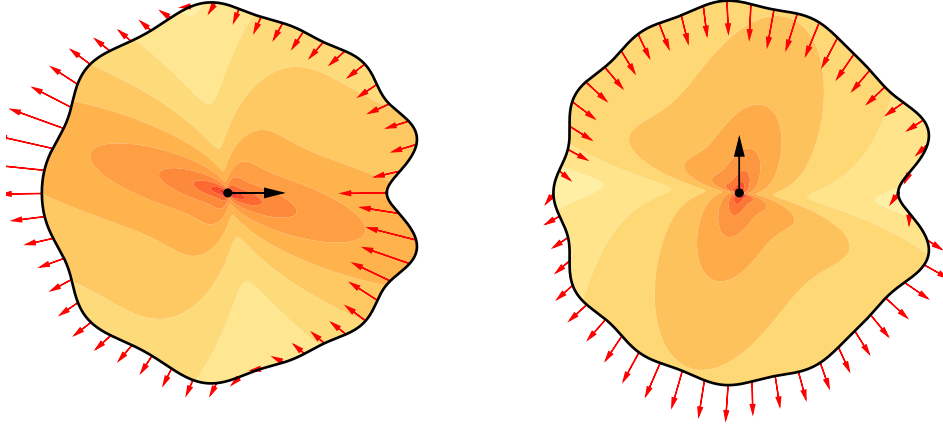


Figure 7: Equilibrated traction fields on random curves in an orthotropic plane subjected to a concentrated force \underline{e}_1 (on the left) and \underline{e}_2 (on the right).

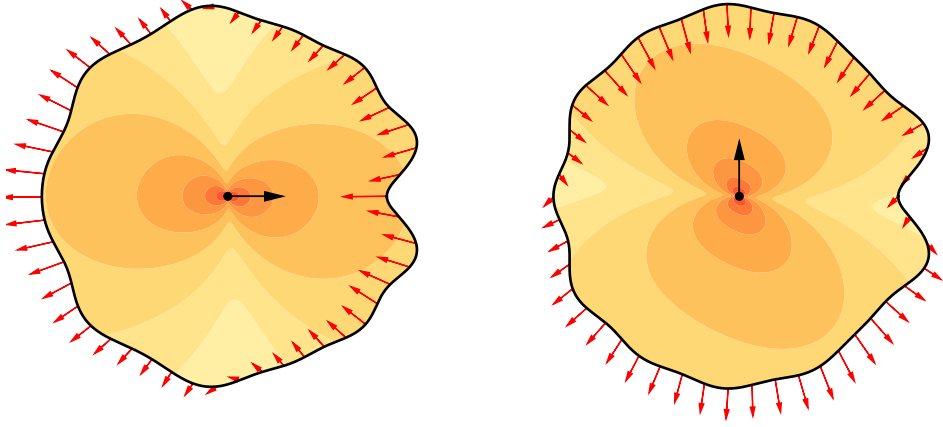


Figure 8: Equilibrated traction fields on random curves in a R0-orthotropic plane subjected to a concentrated force \underline{e}_1 (on the left) and \underline{e}_2 (on the right).

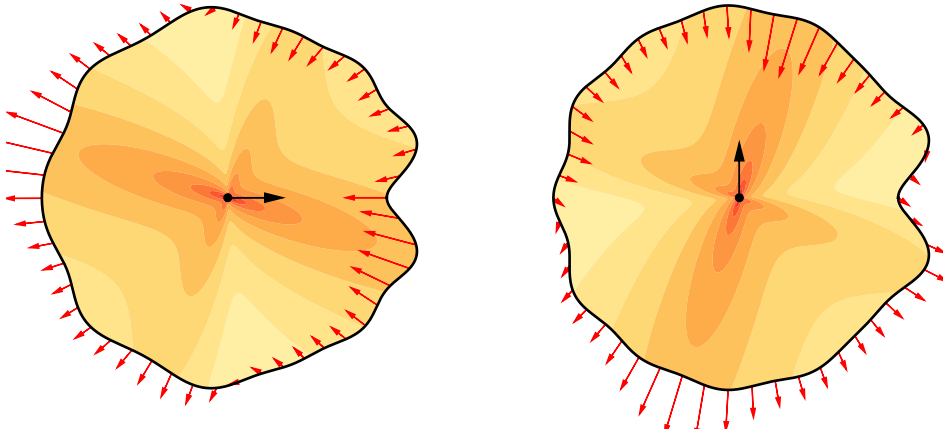


Figure 9: Equilibrated traction fields on random curves in a square-symmetric plane subjected to a concentrated force \underline{e}_1 (on the left) and \underline{e}_2 (on the right).

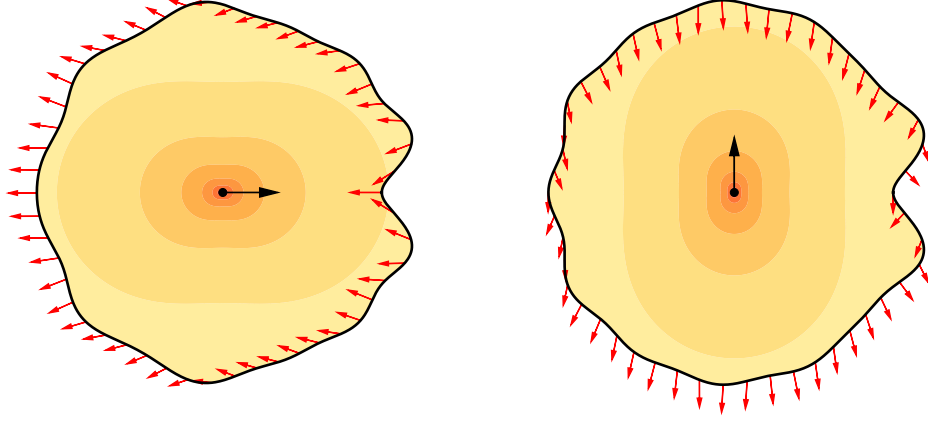


Figure 10: Equilibrated traction fields on random curves in an isotropic plane subjected to a concentrated force \underline{e}_1 (on the left) and \underline{e}_2 (on the right).

9 Conclusion

A recursive method was developed, implemented and verified for the computation of the gradients of 2D anisotropic elastic Green's functions. The approach proposed relies on the Barnett-Lothe integral formalism which proposes robust solutions of the displacement field of anisotropic planes subjected to concentrated forces and dislocations. For square symmetric, R0-orthotropic, orthotropic and anisotropic media, the complete Barnett-Lothe integrals are computed numerically while analytical expressions of the derivatives of the Barnett-Lothe integrands were derived and implemented analytically. The recursive algorithm makes use of those expressions to compute gradients up to the eighth order, at the moment. Verifications of the method were successfully carried over both analytically and numerically. The computation of the gradients of the Green's functions will now be used to implement our first estimates of stationary high order polynomial polarization stress fields of the Hashin-Shtrikman functional of heterogeneous anisotropic elastic media.

References

- Bacon, D., Barnett, D., and Scattergood, R. (1980). Anisotropic continuum theory of lattice defects. *Progress in Materials Science*, 23:51 – 262.
- Barnett, D. and Lothe, J. (1973). Synthesis of the sextic and the integral formalism for dislocations, greens functions and surface waves in anisotropic elastic solids. *Phys. Norv.*, 7:13–19.
- Barnett, D. M. (1972). The precise evaluation of derivatives of the anisotropic elastic green’s functions. *physica status solidi (b)*, 49(2):741–748.
- Brisard, S., Dormieux, L., and Sab, K. (2014). A variational form of the equivalent inclusion method for numerical homogenization. *International Journal of Solids and Structures*, 51(3):716 – 728.
- Eshelby, J., Read, W., and Shockley, W. (1953). Anisotropic elasticity with applications to dislocation theory. *Acta Metallurgica*, 1(3):251 – 259.
- Hayes, M. (1972). Connexions between the moduli for anisotropic elastic materials. *Journal of Elasticity*, 2(2):135–141.
- Lee, V. (2009). Derivatives of the three-dimensional green’s functions for anisotropic materials. *International Journal of Solids and Structures*, 46(1819):3471 – 3479.
- Sales, M. A. and Gray, L. J. (1998). Evaluation of the anisotropic greens function and its derivatives. *Comput. & Struct*, 69:247–254.
- Stroh, A. N. (1958). Dislocations and cracks in anisotropic elasticity. *Philosophical Magazine*, 3(30):625–646.
- Stroh, A. N. (1962). Steady state problems in anisotropic elasticity. *Journal of Mathematics and Physics*, 41(1-4):77–103.
- Synge, J. (1957). *The hypocircle in mathematical physics: A method for the approximate solution of boundary value problems*. Cambridge University Press.
- Ting, T. (1996). *Anisotropic Elasticity: Theory and Applications*. Oxford University Press.
- Vannucci, P. (2009). Influence of invariant material parameters on the flexural optimal design of thin anisotropic laminates. *International Journal of Mechanical Sciences*, 51(3):192 – 203.
- Vannucci, P. (2016). *Another View on Planar Anisotropy: The Polar Formalism*, pages 489–524. Springer International Publishing, Cham.
- Willis, J. (1975). The interaction of gas bubbles in an anisotropic elastic solid. *Journal of the Mechanics and Physics of Solids*, 23(2):129 – 138.